

# MONTHLY WEATHER REVIEW

JAMES E. CASKEY, JR., Editor

Volume 91, Number 5

Washington, D.C.

MAY 1963

## NUMERICAL TROPOSPHERIC PREDICTION WITH A DIVERGENT BAROTROPIC MODEL<sup>1</sup>

G. J. HALTNER

U.S. Naval Postgraduate School, Monterey, Calif.

LT. HARRY E. NICHOLSON, USN

Fleet Numerical Weather Facility, Monterey, Calif.

LT. WINSLOW B. OAKES, USN

U.S. Naval Postgraduate School, Monterey, Calif.

[Manuscript received November 23, 1962; revised February 15, 1963]

### ABSTRACT

An empirically adjusted equation based primarily on Årnason's quasi-barotropic stratified model is used to predict the heights of the 300-, 500-, 700- and 850-mb. levels. The model shows moderate success and appears to fulfill its intended aim of providing useful prediction of the movement of pressure systems. No mechanism is provided for significant development and this mainly accounts for the errors in prediction.

### 1. INTRODUCTION

In spite of its simplicity, the barotropic model for numerical prediction has had remarkable success at 500 mb. On the other hand, the baroclinic models, their greater sophistication notwithstanding, generally have not been as successful at 500 mb. nor have they been quite as satisfactory at other levels as conventional methods for the prognosis of the pressure-height field. The primary reason for the failure of the baroclinic models appears to lie in an inadequately controlled development mechanism. Årnason [1] recently presented the so-called stratified model with the aim of providing "realistic displacements of pressure systems . . . but containing no mechanism for development."

The purpose of this investigation is to apply an empirically adjusted quasi-barotropic prediction equation to several pressure levels below and above 500 mb. The prediction equation is based primarily on Årnason's development, but also partially on the "equivalent

barotropic" concept [2]. Where parameters in the model are not easily identified with their counterparts in the actual atmosphere, empirical values are determined so as to optimize the forecasts.

### 2. THEORETICAL BASIS

An approximate form of the vorticity equation often used in numerical forecasting is

$$\frac{\partial \zeta}{\partial t} + \mathbf{V} \cdot \nabla (\zeta + f) = f_m \frac{\partial \omega}{\partial p} \quad (1)$$

where  $f_m$  represents the mean Coriolis parameter and the other notation is as usual. In the equivalent barotropic model the wind is assumed to be of the form

$$\mathbf{V} = A(p) \hat{\mathbf{V}}, \quad (2)$$

where the symbol  $\hat{\mathbf{V}}$  denotes the vertically integrated mean with respect to pressure. It follows from (2) that the vorticity is

$$\zeta = A(p) \hat{\zeta} \quad (3)$$

<sup>1</sup> This research was supported in part by the Office of Naval Research.

Substituting (2) and (3) into (1) and integrating with respect to pressure lead to

$$\frac{\partial \hat{\zeta}}{\partial t} + \hat{\mathbf{V}} \cdot \nabla (\hat{A}^2 \hat{\zeta} + f) = 0 \quad (4)$$

Defining  $\mathbf{V}^* = \hat{A}^2 \hat{\mathbf{V}}$ ,  $\zeta^* = \hat{A}^2 \hat{\zeta}$  and substituting these quantities into (4) gives the familiar equivalent barotropic forecasting equation. On the other hand, substituting (2) and (3) back into (4) gives

$$\frac{\partial \zeta}{\partial t} + \mathbf{V} \cdot \nabla (K_1 \zeta + f) = 0 \quad (5)$$

where  $K_1 = \hat{A}^2 / A$ . This equation, within the limits of the model, presumably applies at any level with the appropriate  $K_1$ .

In the stratified model the atmosphere is compressible and the disturbances are allowed to vary with height; however the basic current  $U$  is assumed constant. Analytical solutions of the linearized equations lead to the following expression for the horizontal divergence

$$-\frac{1}{g'H} \left( \frac{\partial \phi'}{\partial t} + U \frac{\partial \phi'}{\partial x} \right) \quad (6)$$

Here  $g'$  is a measure of gravity dependent on static stability,  $\phi'$  is the perturbation geopotential, and  $H$  is the vertical distance between the upper and lower rigid boundaries. For application to a non-linear prediction equation, Arnason replaces (6) by

$$-\frac{f}{g'H} \left( \frac{\partial \psi}{\partial t} + \bar{\mathbf{V}} \cdot \nabla \psi \right), \quad (7)$$

where  $\psi$  is a stream function to be obtained from, say, the balance equation; and  $\bar{\mathbf{V}}$  is some sort of zonal or space-mean wind. Substituting (7) into the vorticity equation (1) in place of  $-\partial\omega/\partial p$  leads to the prediction equation

$$\left( \nabla^2 - \frac{f\eta}{g'H} \right) \frac{\partial \psi}{\partial t} + \mathbf{V} \cdot \nabla \eta - \frac{f\eta}{g'H} \bar{\mathbf{V}} \cdot \nabla \psi = 0 \quad (8)$$

Here the absolute vorticity  $\eta$  appears instead of the approximation  $f_m$ . This vorticity equation is similar to that given by Cressman [3] and Wiin-Nielsen [4], except for the last term, which Arnason indicated may give better control over the displacement of the planetary waves. This conclusion is based on the frequency equation which shows that the  $\beta$  term may be suppressed by proper choice of the parameter  $g'H$ . Also the last term in (8) represents advection of the stream field by the mean wind, thus introducing a "steering" influence, and suggests the possibility of application to other levels below 500 mb.

The parameter  $g'H$  has no exact counterpart in the atmosphere, hence it was chosen empirically so that the coefficient of the Helmholtz term is the same as that used by Cressman [3], namely,  $g'H = gH_5 f / 4f_m$ , where  $H_5$  is the standard height of the 500-mb. surface. It is well known that this particular value gives adequate control of the

planetary waves at 500 mb. In Arnason's model, the basic current was constant; however, in the actual atmosphere, the zonal wind varies with height. Hence the interpretation of  $\bar{\mathbf{V}}$  is open to selection on purely utilitarian grounds. On the basis of the empirical considerations involved in the two independent equations (5) and (8) for quasi-barotropic prediction, the following combination was chosen for testing purposes:

$$\left( \nabla^2 - \frac{4f_m\eta}{gH_5} \right) \frac{\partial \psi}{\partial t} + \mathbf{V} \cdot \nabla (K_1 \zeta + f) - K_2 \frac{4f_m\eta}{gH_5} \bar{\mathbf{V}} \cdot \nabla \psi = 0 \quad (9)$$

The coefficients  $K_1$ ,  $K_2$ , and the mean wind  $\bar{\mathbf{V}}$  were to be chosen so as to optimize pressure-height prediction at various levels in the sense of minimum root-mean-square-error.

### 3. PROCEDURES AND RESULTS

Equation (9) was solved over the U.S. Fleet Numerical Weather Facility's (FNWF) 1977-point octagonal grid, covering the Northern Hemisphere to about 10° N., on a Control Data Corporation (CDC) 1604 digital computer. The programming was greatly simplified by the use of the FNWF subroutine library.

One series of forecasts was made at 500, 700, and 850 mb. involving a  $\bar{\mathbf{V}}$  obtained from the 500-mb. and 700-mb. levels. A second series was made independently for the 300-mb. level involving only 300-mb. data. In all forecasts, the stream function was first obtained by solution of the balance equation from computer analyzed data.

Prognosis was accomplished in time steps of 1 hr. with the usual central difference analog, except initially and every 12 hr. when a simple forward difference was utilized.

Verification was based on simply a point by point difference between forecast ( $F$ ) and analyzed ( $A$ ) values yielding the "pillow" ( $P$ ) and root-mean-square-error ( $RMSE$ ):

$$P = \frac{1}{N} \sum_{n=1}^N (F_n - A_n); \quad RMSE = \left[ \frac{1}{N} \sum_{n=1}^N (F_n - A_n - P)^2 \right]^{1/2} \quad (10)$$

#### SERIES I

In the first series of forecasts, Arnason's model was adhered to rather closely. The parameter  $K_1$  was taken to be unity and an optimum  $K_2$  was determined for the 500, 700, and 850-mb. levels. The mean wind  $\bar{\mathbf{V}}$  was obtained by first heavily smoothing the 500- and 700-mb. height fields and then forming the weighted average

$$\bar{z} = 0.75\bar{z}_5 + 0.25\bar{z}_7 \quad (11)$$

The geostrophic wind obtained from the  $\bar{z}$  field initially is used for the first 6 hr., and then a new  $\bar{\mathbf{V}}$  is computed from the forecast fields for the next 6 hr., etc.

The parameter  $K_2$  was varied from 2 to 5 at 850 mb., 1 to 4 at 700 mb., and 0 to 2 at 500 mb. for three randomly chosen days, November 4, 1961, January 20, 1962, and

TABLE 1.—Root-mean-square-error (*RMSE*) for 24- and 48-hr. forecasts at 850, 700, and 500 mb. for optimum values of  $K_2$  at each level

	850 mb. <i>RMSE</i> (ft.) $K_2=3.5$	700 mb. <i>RMSE</i> (ft.) $K_2=2.75$	500 mb. <i>RMSE</i> (ft.) $K_2=0.9$
24-hr. forecast.....	108	111	146
48-hr. forecast.....	171	170	215

May 6, 1962. Forecasts were made for 24 and 48 hr. and faired, and curves of *RMSE* versus  $K_2$  were constructed. The data were very regular and the curves smooth so that optimum values of  $K_2$  were easily obtained.

Table 1 gives the mean *RMSE* (ft.) for 24- and 48-hr. forecasts for the optimum values of  $K_2$  as listed.

It should be mentioned that the variation of *RMSE* with  $K_2$  for the various values listed earlier ranged from about 5 ft. to about 20 ft.; however, values of  $K_2$  outside this range gave substantially larger *RMSE*'s. Geostrophic forecasts, rather than stream function, were also made, and the *RMSE*'s were about 15 to 20 ft. greater for 24 hr. and 25 to 50 ft. greater for 48 hr.

The individual charts showed that, in general, the eastward speed of the synoptic systems increased with increasing  $K_2$  in middle latitudes. On the other hand, the predicted intensity of the systems did not vary significantly with  $K_2$ . This was expected since, by its very nature, the additional divergence term in (9), peculiar to the stratified model, affects the movement of systems rather than their development.

For the case of May 6, 1962, 1000-mb. forecasts were also made. The *RMSE* versus  $K_2$  curve for this case was essentially parallel to that for 850 mb.; however the *RMSE* was about 10 ft. greater.

SERIES II

A second series of forecasts was made for the 300-mb. level. The first difficulty that arose was that the FNWF method of solution for the balance equation, which works satisfactorily at lower levels, generally, did not converge to the prescribed cut-off criterion, namely, all residuals less than 0.5 ft. It was found that a few points persisted with residuals of 3 to 5 ft.; however, when this was apparent, iteration was halted. This obviously intro-

duces a source of error in the stream function; however, the forecast procedure was continued.

The mean wind for this series was simply a space-averaged wind at 300 mb. obtained by employing the following 4-point smoother 15 times over the finite difference grid:

$$\psi_c = \frac{1}{4}(\psi_N + \psi_S + \psi_E + \psi_W)$$

Here the subscripts designate the points north, south, east, and west of the central point  $c$ .

Table 2 shows the results of varying the factor  $K_2$  with  $K_1$  held equal to unity. Numbers to the left in each column are the pillow and to the right the *RMSE*. For each date the upper numbers correspond to the 24-hr. forecasts, the lower numbers to the 48-hr. forecasts. Values in parenthesis are interpolated values. The balancing errors in the second column give the difference between the height field obtained by balancing and reverting again to height and the initial height field. These values indicate a considerable portion, from 17 percent to 40 percent, of the forecast error. In this connection the final conversion from stream function back to height is unnecessary if only the wind field is desired.

Another series of tests not included here indicated that positive values of  $K_2$  at 300 mb. definitely gave larger *RMSE* errors than negative values. Since optimum values of the parameters were sought, only one positive value of  $K_2$  was tested in this series, and as before, gave substantially larger errors. For the negative values listed, the range of error is not great but the table shows a definite minimum error in the neighborhood of  $K_2 = -1$ . Considering that these samples were from the winter season, and that the balancing error averages 63 ft., the average *RMSE* of 256 ft. shows moderate success for the 300-mb. level.

Table 3 gives the *RMSE* as a function of  $K_1$  for some specific values of  $K_2$ . The *RMSE* is minimum at  $K_1 = 0.9$ ; however the improvement over the normal value of unity is slight. Smaller values of  $K_1$ , ( $K_1 = \hat{A}^2/A$ ; see equation (5)), may well have been expected to be optimum at 300 mb.; however table 2 definitely indicates larger errors, for example, at  $K_1 = 0.7$ .

TABLE 2.—Pillow (left) and root-mean-square-error (*RMSE*) (right) in feet as functions of  $K_2$  for 24-hr. (upper) and 48-hr. (lower) 300-mb. forecasts

Date	Balancing Errors	$K_2$								
		+1.25	-0.5	-0.75	-1.0	-1.25	-1.5	-1.75		
Dec. 14, 1961.....	+9 59	+28 292	(287)	+29 283	+29 280	+29 280	+29 282			
Dec. 15, 1961.....	+14 52	+25 452	(436)	+23 422	+23 412	+23 405	+23 403			
Jan. 13, 1962.....	+39 91	+21 284	(275)	+20 268	+20 263	+20 261	+20 260			
Jan. 17, 1962.....	+26 63	-2 405	(386)	-2 371	-1 360	-1 353	-1 351			
Jan. 21, 1962.....	+12 50	+50 221	+50 222	+50 225	(230)	+49 238	(251)			
Averages.....	63	+44 337	+43 335	+42 338	(346)	+41 358	(377)			
		+14 316	+13 255	+13 255	+13 258	(265)	(276)			
		+58 494	(356)	+59 385	+60 376	+60 391	(404)	(428)		
			(256)	+10 250	+10 248	+10 249	+10 251	(256)		
			(393)	+24 391	+24 391	+24 394	+24 402	(419)		
			262.2	257.8	255.8	256.0	259.0	265.0		
			394.6	386.6	381.6	378.6	384.4	395.6		

TABLE 3.—Pillow (left) and root-mean-square-error (RMSE) (right) in feet as functions of  $K_1$  for specific values of  $K_2$  for 24-hr. (upper) and 48-hr. (lower) 300-mb. forecasts

Date	$K_2$	$K_1$								
		1.0		0.9		0.8		0.7		
Dec. 14, 1961.....	-1.5	+29	280	+29	277	+30	280	+30	287	
		+23	405	+27	389	+31	383	+34	388	
Dec. 15, 1961.....	-1.75	+20	260	+21	259	+22	266			
		-1	351	0	349	+1	358			
Jan. 13, 1962.....	-0.5	+50	221	+51	221	+51	228			
		+44	337	+45	331	+46	335			
Jan. 17, 1962.....	-1.0	+13	255	+13	255	+13	261	( $K_1=0.75$ )	+13	267
		+60	386	+61	384	+61	388		+61	394
Jan. 21, 1962.....	-1.0	+10	248	+10	246	+11	252			
		+24	391	+24	390	+23	403			

For both series of tests the individual charts were examined for the purpose of detecting any characteristic errors. In general, the predicted movement of the system was in good agreement with the observed movement, and the main source of error lay in changes of intensity.

4. SOME SAMPLE FORECASTS

Figures 1 to 3 illustrate one of the 300-mb. forecasts. The 300-mb. contours for 0000 GMT, January 13, 1962 and 0000 GMT, January 14, 1962 are shown in figures 1 and 2. Figure 3 shows a 24-hr. forecast (with  $K_2=-1$ ) made from the 0000 GMT, January 13 machine analysis. Superimposed on the prognostic map are the initial positions (dashed) of the more easily identified troughs and

ridges as obtained from figure 1 and the observed positions (dot-dashed) 24 hr. later from figure 2. The forecast of the short-wave trough in the central Pacific Ocean was in good agreement with the observed movement. Also the intensity of the system was virtually unchanged, hence the error in the pressure-height forecast was near zero here.

The strong ridge in the eastern Pacific Ocean moved only a short distance and the forecast position in the northern and southern portions was good; however the central portion moved somewhat faster than was predicted. Also some of the details in the vicinity of southwestern Alaska were missed. The forecast positions of two short-wave troughs affecting the United States were in good agreement with the machine analysis. However, deepening off the east coast resulted in height errors of about 400 ft.

In the Atlantic Ocean the systems were somewhat less distinct, though there appears to be a weak ridge in the central Atlantic which moved to a position just west of the British Isles. The predicted movement was less than observed in this area and the ridge is somewhat sharper than actually occurred. But the southern extension of the ridge appears in about the same position on both the prognostic and observed maps.

The position of the trough extending from the North Sea to the central Mediterranean Sea and then westward appears to be quite well predicted, although deepening in the eastern Mediterranean resulted in pressure-height

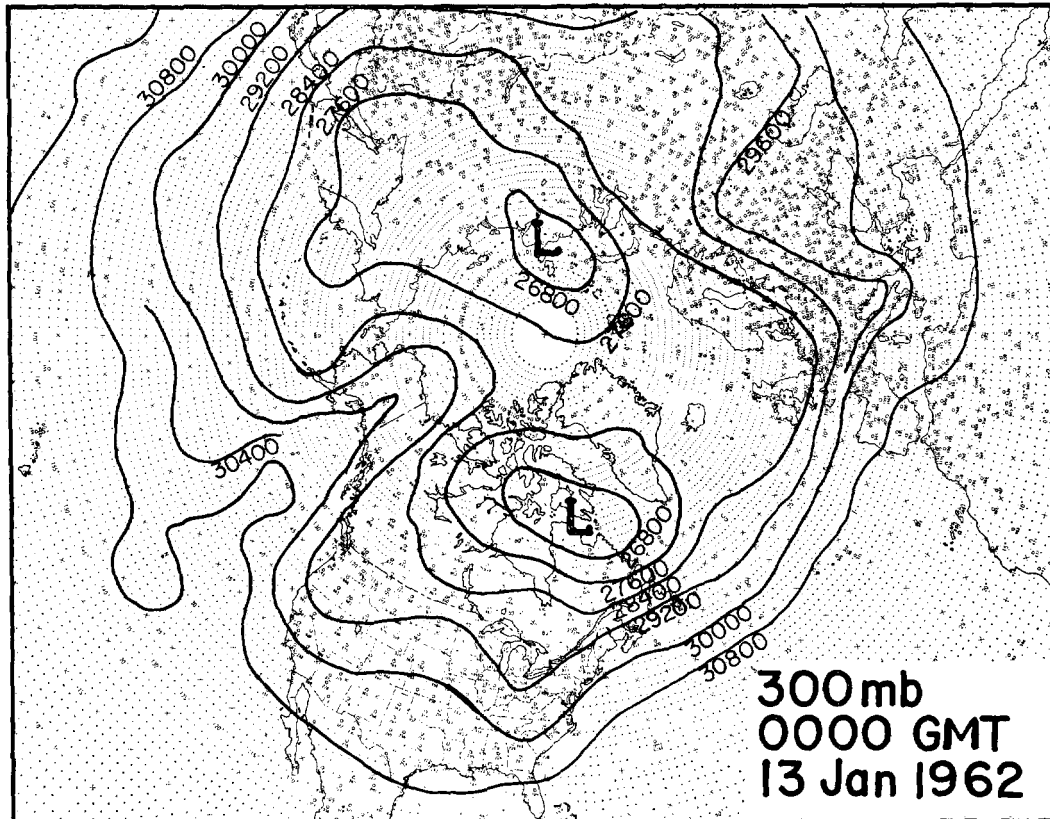


FIGURE 1.—300-mb. analysis for 0000 GMT, January 13, 1962.

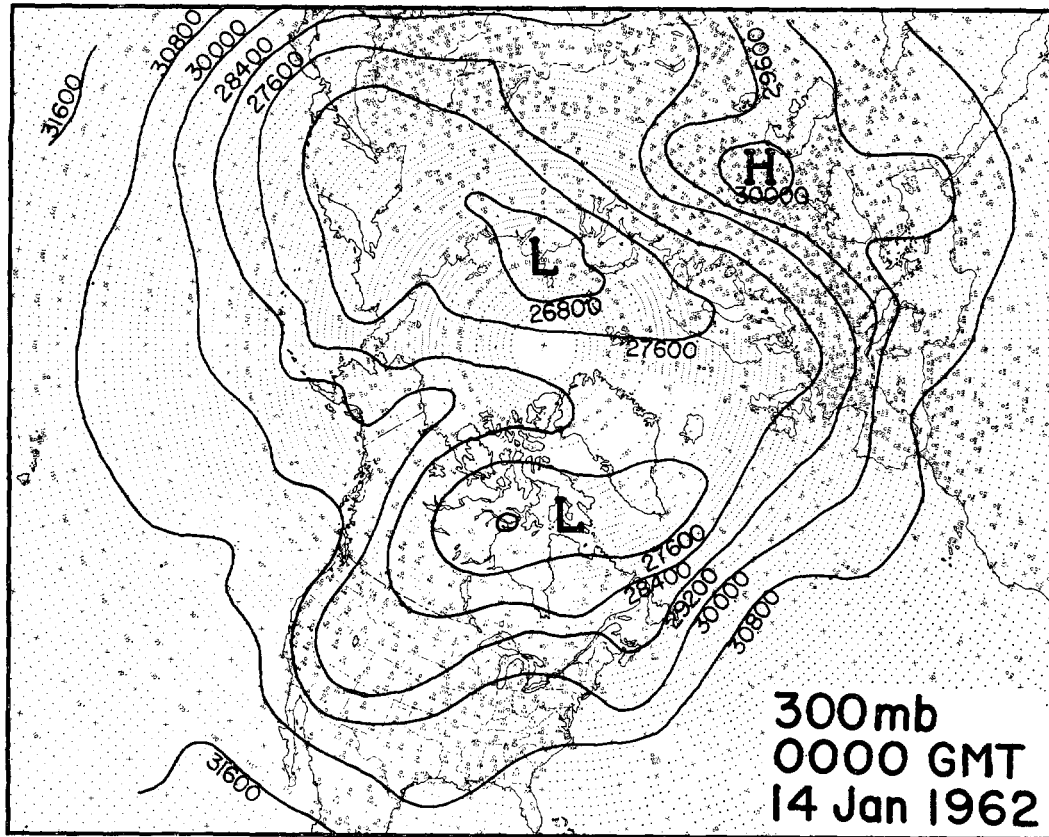


FIGURE 2.—300-mb. analysis for 0000 GMT, January 14, 1962.

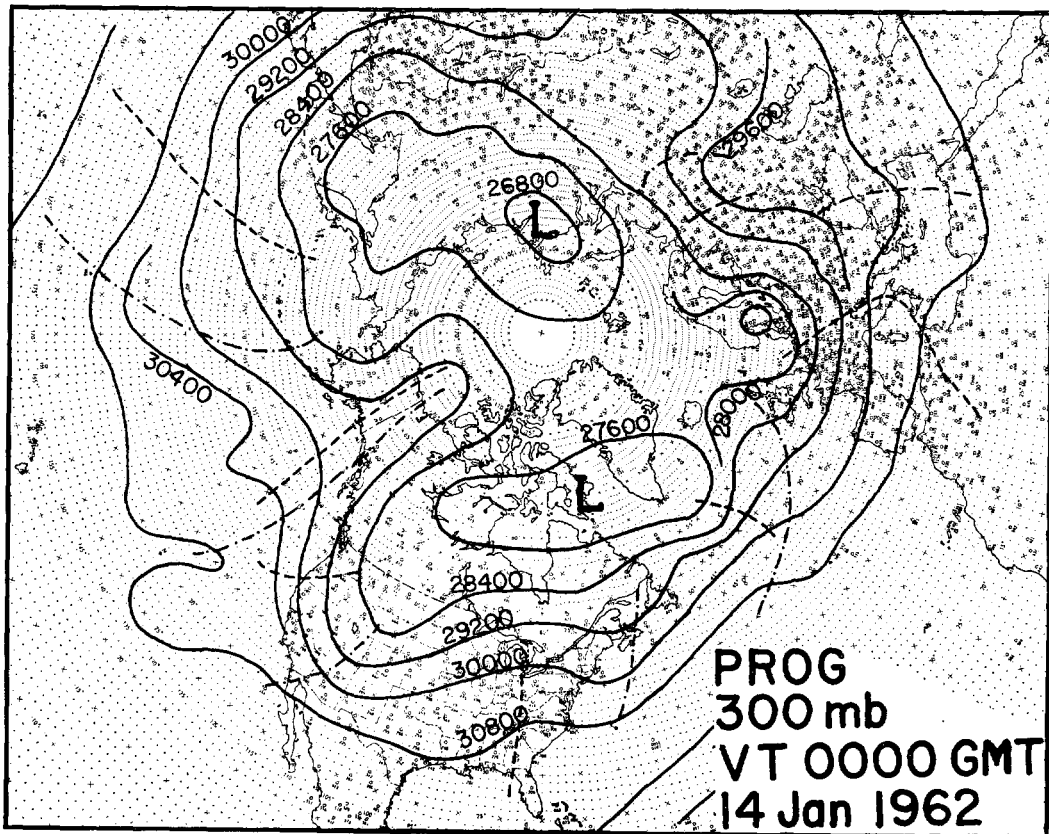


FIGURE 3.—24-hr., 300-mb. prognostic chart with  $K_2 = -1$ , verifying at 0000 GMT, January 14, 1962. Dashed lines represent initial positions of troughs and ridges, and dot-dashed lines represent observed positions.

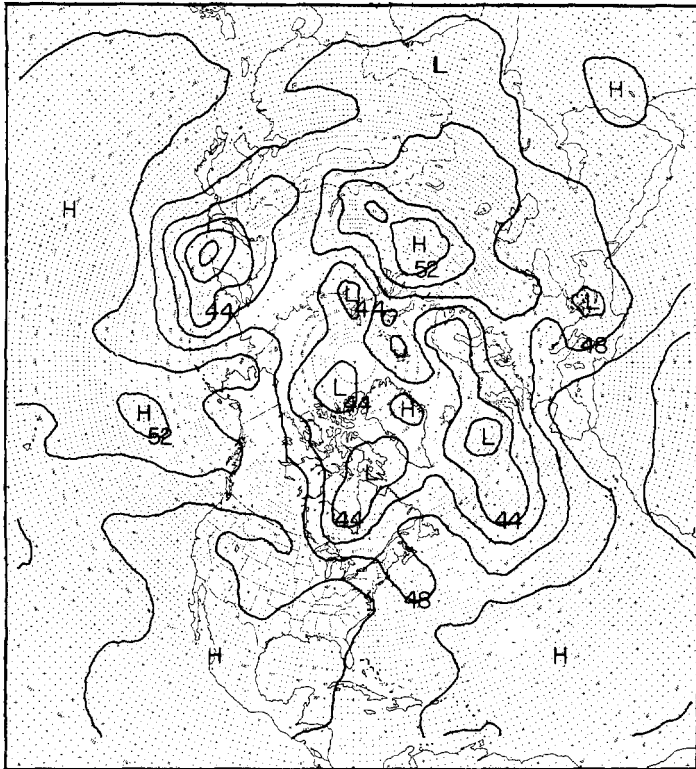


FIGURE 4.—850-mb. analysis for 0000 GMT May 6, 1962. Contour heights in hundreds of feet.

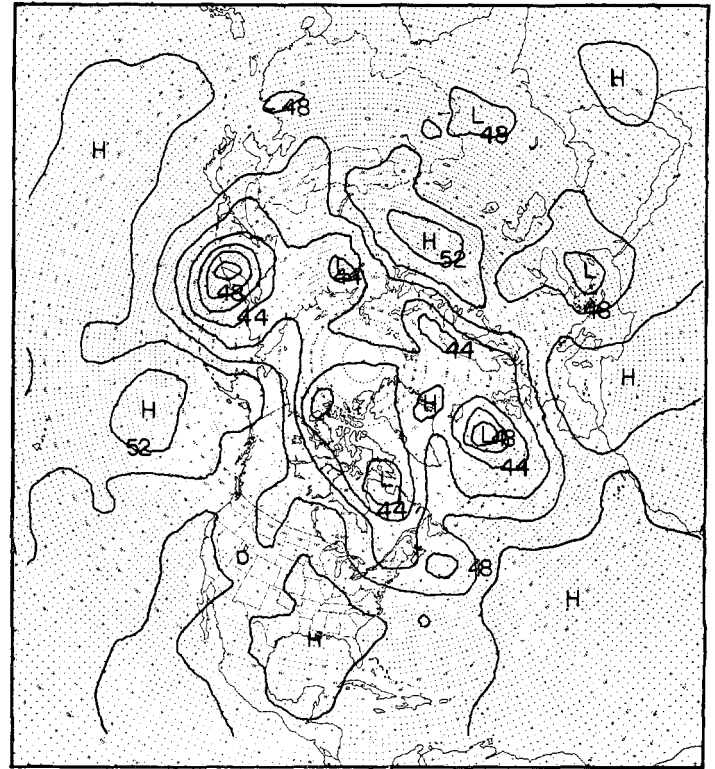


FIGURE 5.—850-mb. analysis for 0000 GMT, May 7, 1962.

errors of nearly 600 ft. Finally, the ridge position in eastern Europe is quite well located.

In summary, the example appears to substantiate the conclusion that the model can provide a good estimate of the movement of systems at the 300-mb. level. Of course, the model provides no mechanism for baroclinic development, and large pressure-height errors may result from this process.

A sample forecast of 850 mb. is shown in figures 4 through 8. Figures 4, 5, and 6 are the 850-mb. analyses for 0000 GMT, May 6, May 7, and May 8, 1962, respectively. The 24- and 48-hr. forecast charts, made (with  $K_2=3$ ) from 0000 GMT, May 6, are shown in figures 7 and 8. Although the continuity of individual troughs and ridges is somewhat more difficult to establish at 850 mb., an attempt has been made to show movement as in the 300-mb. case.

The trough over eastern Canada which extends from southern Hudson Bay to Lake Superior on the initial analysis was moved too slowly for the first 24 hr., but at the end of 48 hr. was well placed. The movement of the ridge immediately ahead of the trough was also correctly forecast. The low center west of Scotland was predicted to remain stationary, as it did, while the trough to the south of the center was advanced correctly, except in the southern portion where the movement was too slow.

In the Pacific, the Low over the Kuriles on the initial chart was forecast to move northeast along the east coast

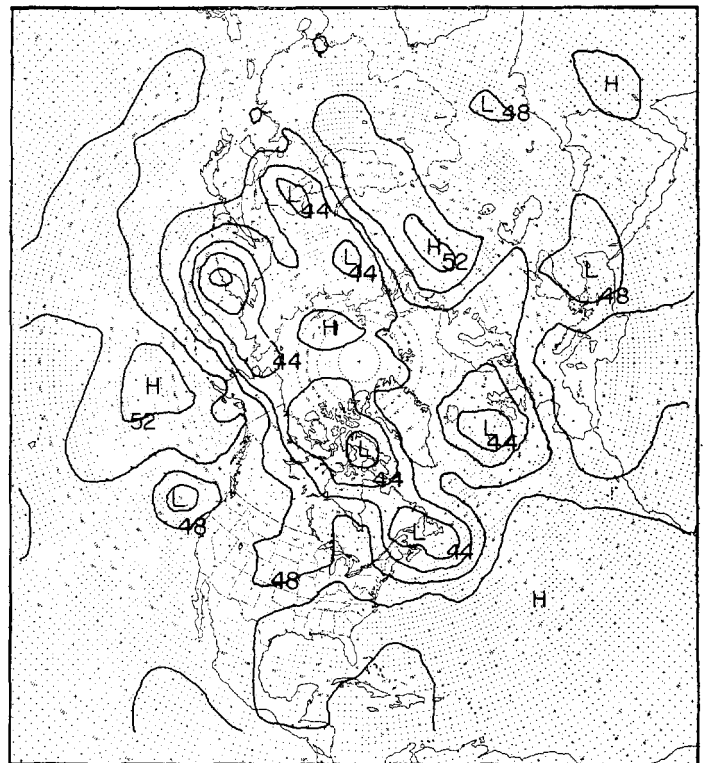


FIGURE 6.—850-mb. analysis for 0000 GMT, May 8, 1962.



FIGURE 7.—24-hr., 850-mb. prognostic chart with  $K_2=3$ , verifying at 0000 GMT, May 7, 1962. Dashed lines represent initial positions of troughs and ridges and the dot-dashed lines represent observed positions.



FIGURE 9.—Velocity divergence in units of  $10^{-6} \text{ sec.}^{-1}$  at 850 mb. for 0000 GMT January 20, 1962 as computed by equation (12)

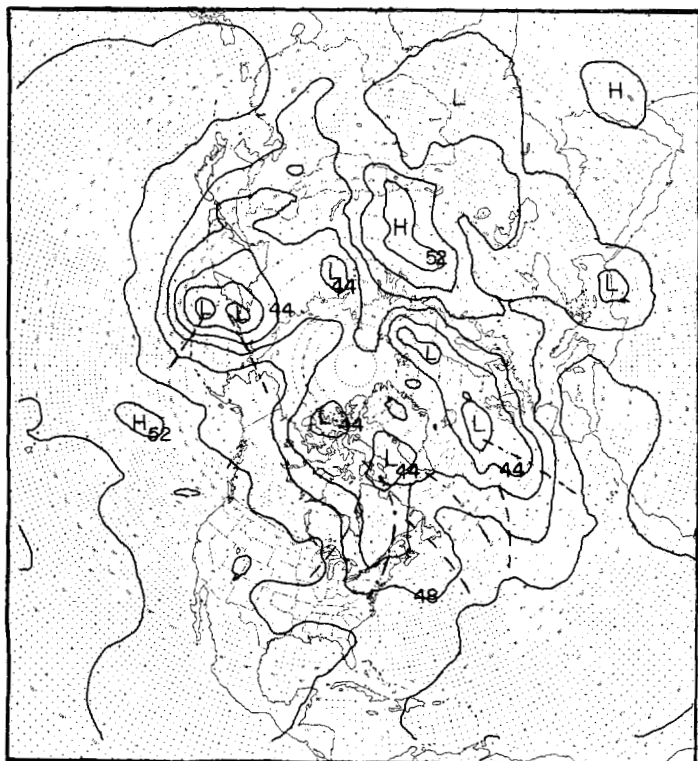


FIGURE 8.—48-hr., 850-mb. prognostic chart with  $K_2=3$ , verifying at 0000 GMT, May 8, 1962. Dashed lines represent initial positions of troughs and ridges and the dot-dashed lines represent observed positions.

of the Kamchatka Peninsula. This prognosis was reasonably good for the first 24 hr., with only a slight error in direction; however, the forecast for the second 24-hr. period continued this movement, while the Low actually became stationary over the southern tip of the Peninsula. The trough which moved north around this center from an initial position over the western Aleutians was placed very well on both the 24- and 48-hr. forecasts, but its forecast intensity was greatly in error because the ridge over western Alaska was not forecast to weaken as actually occurred. On the other hand, the movement of this ridge was predicted quite well.

It may be of some interest to show an example of the velocity divergence implied by the vorticity equation (9) of this model, namely,

$$\nabla \cdot \mathbf{V} = \frac{-4f_m}{gH_3} \left( \frac{\partial \psi}{\partial t} + K_2 \bar{\mathbf{V}} \cdot \nabla \psi \right) \quad (12)$$

Values of divergence were computed with the above expression at the 850-mb. level for 0000 GMT, January 20, 1962, as shown in figure 9. The range of values is approximately  $\pm 5 \times 10^{-6} \text{ sec.}^{-1}$ . Examination of the corresponding height fields revealed that lines of zero divergence correspond very closely to the short-wave trough and ridge lines. Centers of maximum convergence and divergence tend to lie, respectively, between the trough and downwind ridge, and vice versa. Hence, the

divergence field contributes primarily to movement of these systems rather than development.

### 5. SUMMARY AND CONCLUSIONS

An empirically modified equation based primarily on Árnason's quasi-barotropic stratified model has been applied to predict the height field of the 300-, 500-, 700-, and 850-mb. levels. The model appears to fulfill its intended purpose of providing realistic prediction of the displacement of pressure systems to the synoptic forecaster. The largest errors in prediction were concomitant with changes of intensity of the systems. At 500 mb. the

model showed a slight improvement over the conventional divergent one-parameter model.

### REFERENCES

1. G. Árnason, "A Study of the Dynamics of a Stratified Fluid in Relation to Atmospheric Motions and Physical Weather Prediction," *Tellus*, vol. 13, No. 2, May 1961, pp. 156-170.
2. J. G. Charney, "On a Physical Basis for Numerical Prediction of Large-Scale Motions in the Atmosphere," *Journal of Meteorology*, vol. 6, No. 6, Dec. 1949, pp. 371-385.
3. G. P. Cressman, "Barotropic Divergence and Very Long Atmospheric Waves," *Monthly Weather Review*, vol. 86, No. 8, Aug. 1958, pp. 293-297.
4. A. Wiin-Nielsen, "On Barotropic and Baroclinic Models, with Special Emphasis on Ultra-Long Waves," *Monthly Weather Review*, vol. 87, No. 5, May 1959, pp. 171-183.